J Nanostruct 10(4): 713-722, Autumn 2020

RESEARCH PAPER

# HRTEM study of ZnS Nanowires Films Deposited by Thermal Evaporation

***B. Abdallah*, M. Kakhia, W. Zetoun***

*Department of Physics, Atomic Energy Commission, Damascus, Syria*

**ARTICLE INFO**

***Article History:***
*Received 11 July 2020*
*Accepted 05 September 2020*
*Published 01 December 2020*

***Keywords:***
*HRTEM*
*Nanowires*
*PbS doped ZnS films*
*Thermal evaporation*

**ABSTRACT**

ZnS nanowires films on Si (100) substrate have been obtained, using PbS as dopant, via thermal evaporation technique. High resolution transmission electron microscopy (HRTEM) images have confirmed the formation of ZnS nanowires. *Energy dispersive* X-ray analysis (EDX) has been employed to investigate the element's contents (mapping and area analysis) and it has confirmed that the ZnS films were stoichiometry. Thickness and morphology of the films were explored from cross section of the films and surface, respectively, using scanning electron microscopy (SEM) and atomic force microscopy (AFM) images. These images confirmed the creation of ZnS nanostructures morphology. The diameter of the obtained nanowires is about 50 nm and their length is several micrometer. Fourier-transform infrared spectroscopy (FTIR), X-Ray Diffraction (XRD), and Photoluminance (PL) have confirmed the hexagonal phase with nanowires structure. UV-Vis characterization has been used to obtain the transparency and the band gap of ZnS films deposited on glass substrate. Also, these verified characterizations allowed to potential optical application in optoelectronic field.

**How to cite this article**
*Abdallah B. , Kakhia M., Zetoun W. HRTEM study of ZnS Nanowires Films Deposited by Thermal Evaporation. J Nanostruct, 2020; 10(4): 713-722. DOI: 10.22052/JNS.2020.04.004*

## INTRODUCTION

ZnS is outstanding semiconductor material, it widely used as a nano-generators, bio-sensors, photo voltaic solar cells [1] and light emitting diode (LED) [2]. Additionally, ZnS is non-toxic material (friend to the environment) and transparent with band gap of 3.4eV, biocompatible, and has biodegradable properties [2]. ZnS have been to be an excellent candidate for potential applications in the optical field of nonlinear modulators [3].

Nanowires, nanotubes and nanoparticles have been emerged as promising candidates for different applications; for example Silver nanostructures is an effective antibacterial materials [4] and Strontium oxides have magnetic applications. Bagher et al [5] has been investigated the crystal structure and magnetic properties of $SrFe_{12}O_{19}$ hexa-ferrites nanoparticles. Also, Eskandari et al [6] has been prepared a new magnetic and photo-catalyst $CoFe_2O_4$–$SrTiO_3$ perovskite nanocomposite. Moreover, Nabiyouni et al [7] has been synthesized mono-disperse platinum nanoparticles and $NiFe_2O_4$@$TiO_2$/Pt nanocomposites by a facile sol-gel procedure.

Normally, doping with different metals would improve and/or modify semiconductor properties such as: ZnS, PbS, ZnO, and $SnO_2$ [8]. The doping processes would induce some modified electronic properties such as transparency and band gap [9, 10]. Moreover, Pb dopant become more interesting compared to other dopants materials due to their lower anisotropic field and fast crystallization process. Pb was chosen as dopants for many different reasons for example: the ionic radius of $Pb^{2+}$(0.119 nm) is higher than $Zn^{2+}$(0.074 nm), this makes Zn more active than Pb during

* *Corresponding Author Email: pscientific27@aec.org.sy*

chemical reaction. Therefore, Pb can substitute $Zn^{2+}$in the ZnS lattice [11].

Abdelkrim et al [10] have correlated the crystallography (grain size and orientation) with the electrical conductivity. Numerous methods can be employed to produce ZnS thin films such as chemical bath deposition (CBD) [12, 13], PLD technique [14], RF magnetron sputtering [15, 16] chemical precipitation method, ultrasonic spray pyrolysis technique [17] and thermal evaporation [18, 19]. The later method is widely used on film production, since it is low cost and simple method. The structural and optical properties of ZnS films are influenced by different parameters like variation of the thickness, grain size and concentration of the dopant element [13, 20].

Morphology can be affected by many parameters such as: substrate temperature [21], concentration [10], film thickness (deposition time) [22], and structure of the film and dopant concentration[23]. The surface morphology, size, form, nanostructure effect on the physical, chemical and electrical properties of thin films have been compared to the bulk behavior especially in semiconducting materials [24]. Recently, Hazra et al [25] have demonstrated the core–shell structure of ZnO films deposited on silicon nanowires (NW) heterostructures with SiNWs as core and ZnO thin film as shell prepared by Atomic Layer Deposition.

ZnS exhibits two different crystal structures zinc blend [26] and wurtzite structures [17] . Nanostructured ZnS has been formed as nanobelts, nanocombs, nanowires and nanohelices using many synthesizing methods [27],[28]. All of these properties would make one-dimensional nanostructured ZnS attractive candidates for use in technologies and devices. Two growth mechanisms "the vapor-solid [29] and vapor-liquid-solid (VLS)" have used to explain nucleation and growth. Amico and coworker investigated doping effects, as induced by Al and Cu, on promoting different ZnS phases using first principles simulations [30].

In this work, we have investigated the growth of doping PbS: ZnS nanowires behavior for different PbS concentrations using thermal evaporation method. XRD technique was used to study the crystallographic properties. EDX was used to determine the films composition. The evolution of morphology was obtained by HRTEM and SEM characterization of the surface morphology. Where, up to our knowledge, this is the first time that ZnS has been treated by thermal evaporation using PbS as dopant in the purpose of obtaining nanowires ZnS films. However, there was a few work has been published regarding the obtained ZnO nanowires/nanotubes with Pb as dopant [31] [26] .

## MATERILAS AND METHODS

Lead sulfide doped zinc sulfide (PbS:ZnS) thin films were prepared on glass and Si(100) substrates using simple thermal evaporation technique. The ZnS powder (high purity) was used as source material. The PbS powder (6 wt %) was added to ZnS (94 wt %), under a vacuum of $10^{-5}$ Torr. The substrate holder heated before deposition to 200°C [22]. Thickness, as well as, thin films morphology were measured by means of SEM ,TSCAN Vega\\XMU model, equipped with EDX to determine the chemical composition of the synthesized films. X-ray Diffraction ( Stoe Transmission X-ray diffractometer Stadi P) has been used for structural properties [22]. The optical properties have been examined using the UV-Vis Shimadzu UV-310PC spectrophotometer of the elaborated films. laser He-Cd (A 325 nm wavelength) a 1m Spex monochromator was used get of the photoluminescence (PL) measurement at room temperature. The Fourier transform infrared (FTIR) spectra of the films were recorded by Jasco 300 E [32] spectrometer with a resolution of 4 $cm^{-1}$. HRTEM with EDX mapping and typical modes were utilized to obtain the elements composition.

## RESULTS AND DISCUSSION

*HRTEM and EDX mapping study large scale*

For further investigation of the microstructure of the product, the HRTEM measurements have been carried out over selected region for individual Pb-doped ZnS NW as shown in Fig. 1-a. TEM observation has shown the structure of ZnS, it looks like as nanowires and not nanotubes structure. Diameters of the obtained nanowires are in the range of 25 nm. And, the length is about several micron (observed by SEM characterization and the length are more than the dimension of TEM images). The surface of NWs looks to be very smooth.

Fig. 1 presents HRTEM mapping images for EDX analysis (b) for Zn element, (c) for S element and (d) for O element. Such very thin ZnS and ZnO nanowires have not often reported in the literature [33-36]. However, most of the

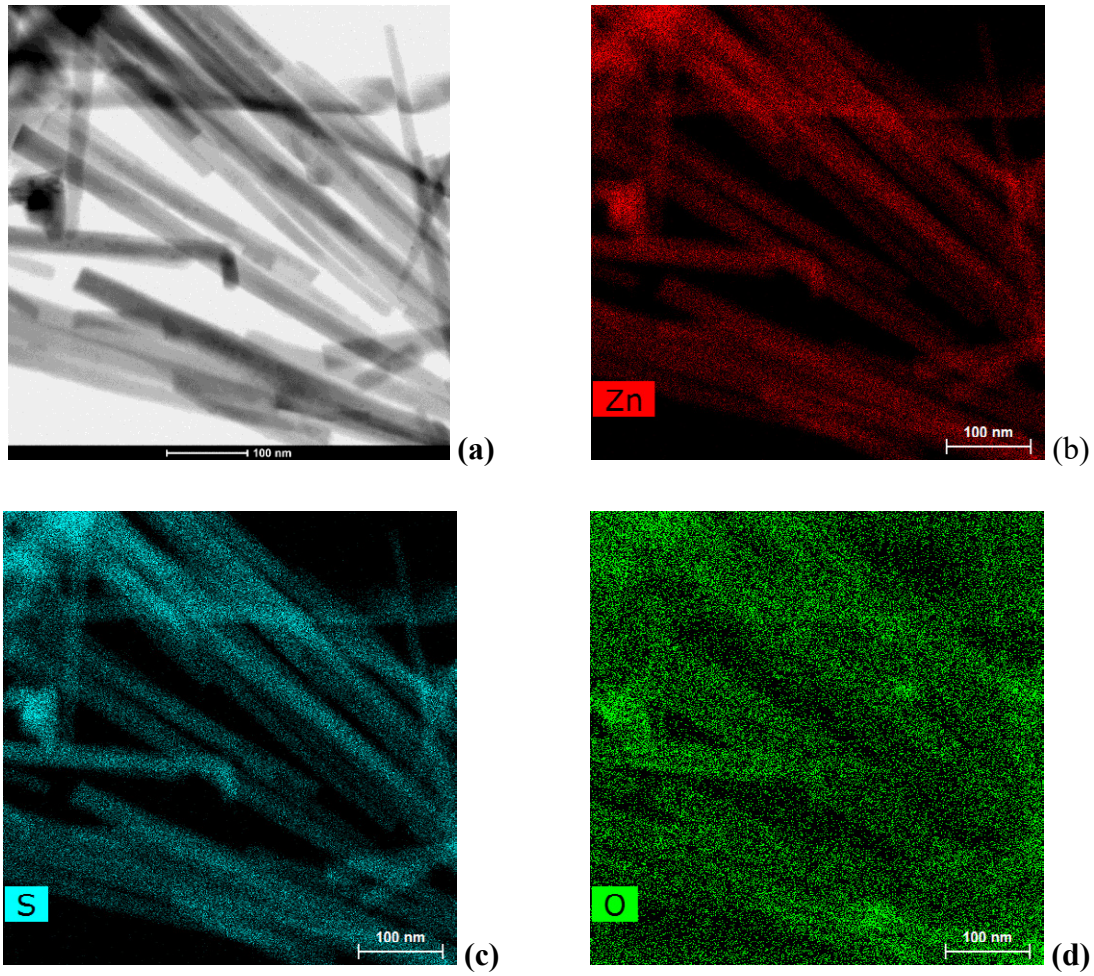


Fig. 1. HRTEM image (a), EDX mapping images (b) Zn element, (c) S element and (d) O element.

synthesizing processes involve more than one step in order to obtain the desired thin NW`s in our case, The synthesis of these NWs was conducted by the simple thermal deposition technique.

EDX mapping was carried out for TEM images (Fig. 1 b, c and d) of Zn, O and S elements, this analysis has confirmed that the nanowires are mainly composited of Zn and S elements. However, the wires are clear and determined, while the O element is low and it is a contamination (small quantity). This result was confirmed in EDX using SEM percentage in next paragraph (less than 6 % atomic percentage).

*HRTEM and EDX mapping study small scale*

Similarly, another zone was selected (HRTEM image (2-a) to verify the structural and the composition of nanowires using mapping EDX (Fig. 2). The diameters are less than 50 nm, the SEM study confirms our results. EDX data using TEM technique shows the elementary composition of nanowires. We have found Zn and S mainly with low percentage of O (b, c and d). This EDX mapping is confirmed that the thermal evaporation techniques is effective method to obtain ZnS nanostructure (nanowires in this selected condition)

The elements percentages for two zones (Fig. 3) are studied using EDX measurements by TEM and are summarized in Table 1. The Si element is due to TEM preparation and to the substrate (Pb:ZnS was deposited on Si(100)), the O element is due to the humidity absorbed by nanowires (because the samples was analyzed after film deposited).

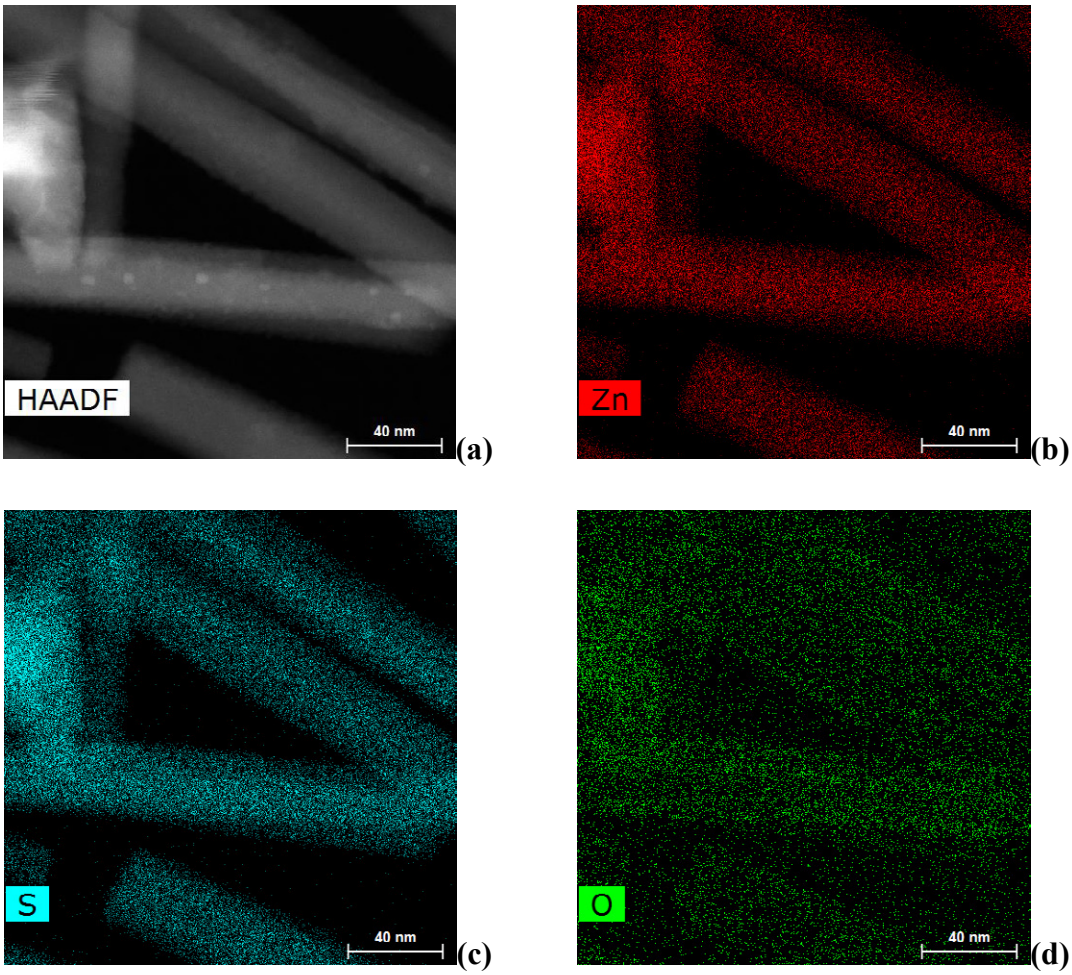


Fig. 2. HRTEM image (a), EDX mapping images (b) Zn element, (c) S element and (d) O element.

Table 1. Atomic percentage for PbS:ZnS film using EDX –TEM for big zone and small zone

| Element | big (at.%) | small (at.%) |
|---|---|---|
| Zn | 40.95671 | 41.08195 |
| S | 38.97932 | 38.82073 |
| O | 16.58584 | 16.77945 |
| Si | 3.478128 | 3.317879 |

*SEM, AFM and EDX study*

SEM was used to investigate the structural morphology of the synthesized products. Fig. 4. shows the morphology of the surface doped ZnS NWs in the sample with different magnifications (a) at 35k magnification). It is clear that the product consists of ultra-thin randomly oriented NWs with uniform diameter in the range of ~20–30 nm and length of several microns as shown in Fig. 4-b at 100 k magnification. For further investigations, cross-sectional SEM images were performed for the same doped sample above, where front view of the NW sidewall is captured and presented in Fig. 4. The morphology of the doped sample indicates the formation of the cantilever-like NWs on top of another thin layer (Fig. 4 b). We expect that, during the deposition process, Pb forms a thin monolayer on top the substrate and down of the nanowires, the PbS was a catalyst, and it played the role essential for nonstructural growth.

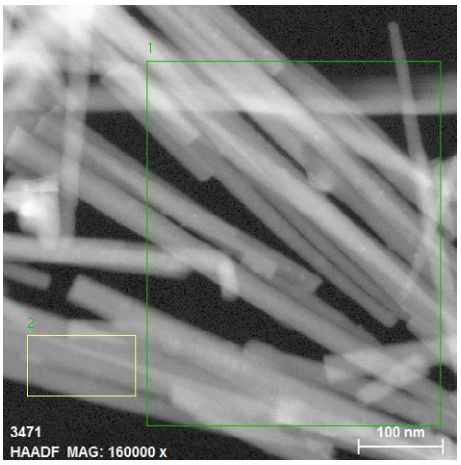


Fig. 3. HRTEM image with two corresponding EDX zones (big zone in green color).

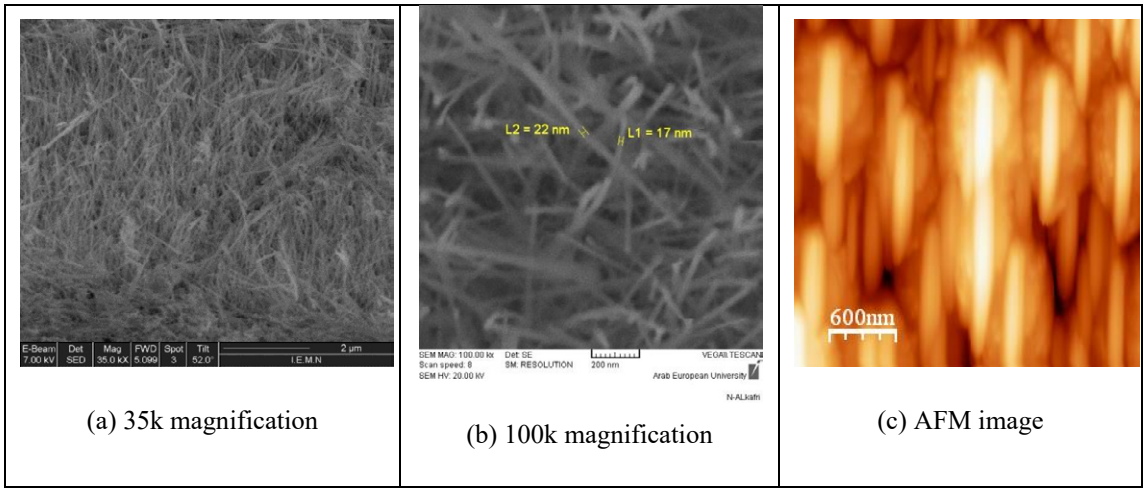


Fig. 4. Surface morphology, (a) and (b) SEM images at 35 k at 100 k magnifications, and (c) AFM image of ZnS nanowires film.

The AFM image shows surface morphology (top view) for ZnS nanowires film at 3x3µm area. This image presents nanostructure of doped ZnS, as shown in Fig. 4-c.

Fig. 5. shows SEM cross section morphology of ZnS nanowires film deposited on Si(100) substrate (a) 20k and (b) at 40 k magnifications secondary electron detector (SE). Also, Fig. 5-c at 40 k magnification using backscattering electron detector (BSE), where this images confirm nanowires growth, Fig. 5-d at 50 k magnification using secondary electron detector (SE).

The SEM (Figs. 4 and 5) and AFM images confirm that the growth as nanowires (was mentioned above ) in TEM studies.

The composition of the PbS;ZnS films was examined firstly by means of EDX (Fig. 6) and the elements percentage was reported in Table 2.

The Weight percentage for Pb is about 5.96 % and the film content mainly Zn and S, so the film is almost stoichiometry and less percentage of O which consider as contamination (less 2 wt %). The next paragraph (XRD and FTIR) will confirm the ZnS structural for nanowires film.

*FTIR, XRD and PL study*

FTIR spectrum of deposited PbS:ZnS/Si film (with doping) in the spectral range 400–4000 $cm^{-1}$ is shown in Fig. 7-a. The peaks near 1120 $cm^{-1}$ are attributed to PbS:ZnS/Si nanowires, this peak was observed in previous work [17], where we are using ultrasonic spray pyrolysis and the

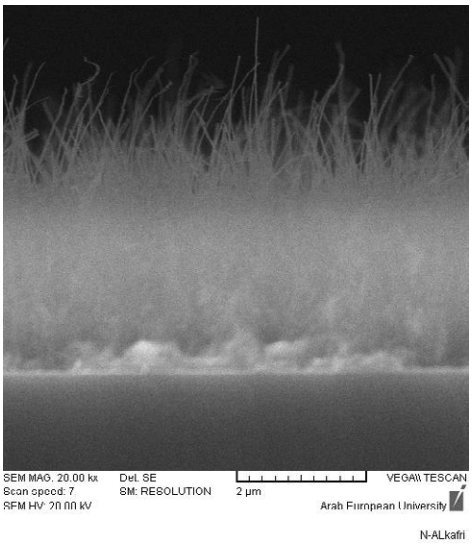


(a) 20k magnification SE detector

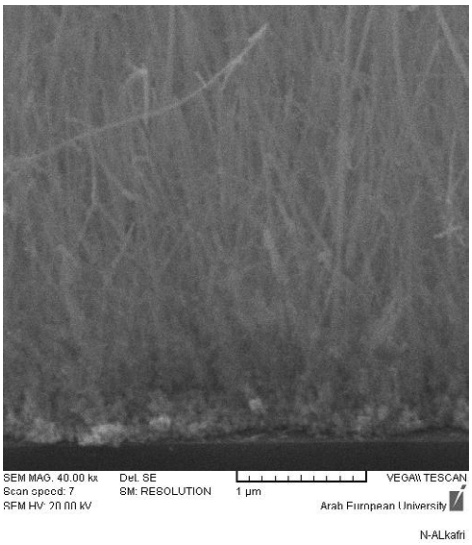


(b) 40k magnification SE detector

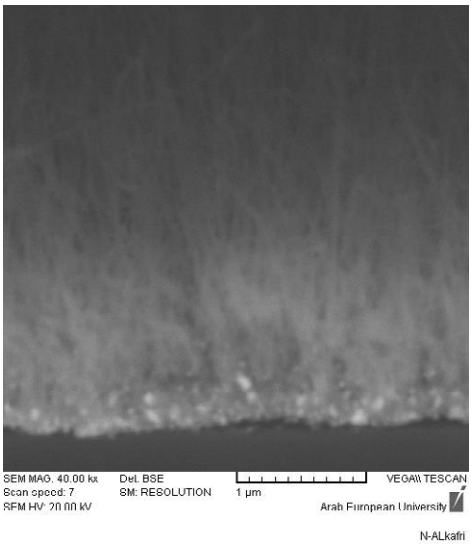


(c) 40k magnification BSE detector

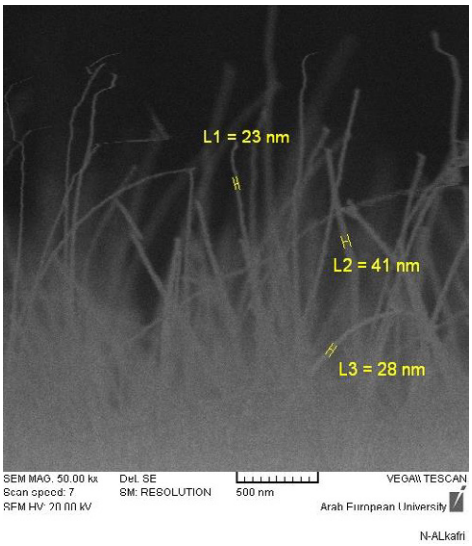


(d) 50k magnification SE detector

Fig. 5. SEM cross section morphology of ZnS nanowires film deposited on Si(100) substrate. (a) 20k and (b) at 40 k magnifications SE detector, (c) at 40 k magnification using BSE detector, (d ) at 50 k magnification using SE detector.

structure was wurtzite hexagonal. While the peak 2350 $cm^{-1}$ is attributed to Si substrate, also the noise between 1300 and 1800 $cm^{-1}$ is due to the presence of atmospheric water in the FTIR system. All peaks were reported in Table 3

XRD pattern shows PbS:ZnS wurtzite hexagonal structure for (PbS doped ZnS film deposited on Si(100)) as shown in Fig. 7-b. The peaks (100), (002), (101) and (110) matching at 26. 92°, 28.55°, 30.50° and 47.55° respectively. These results are in good agreement to the hexagonal phase (wurtzite structure) of ZnS, with PDF Number: 36-1450 with lattice parameters (a=b=3.82 Å and c=6.26 Å).

These results were in accord with recent study, where we obtained ZnS hexagonal structural using spray pyrolysis [37]. But, in last work [38]

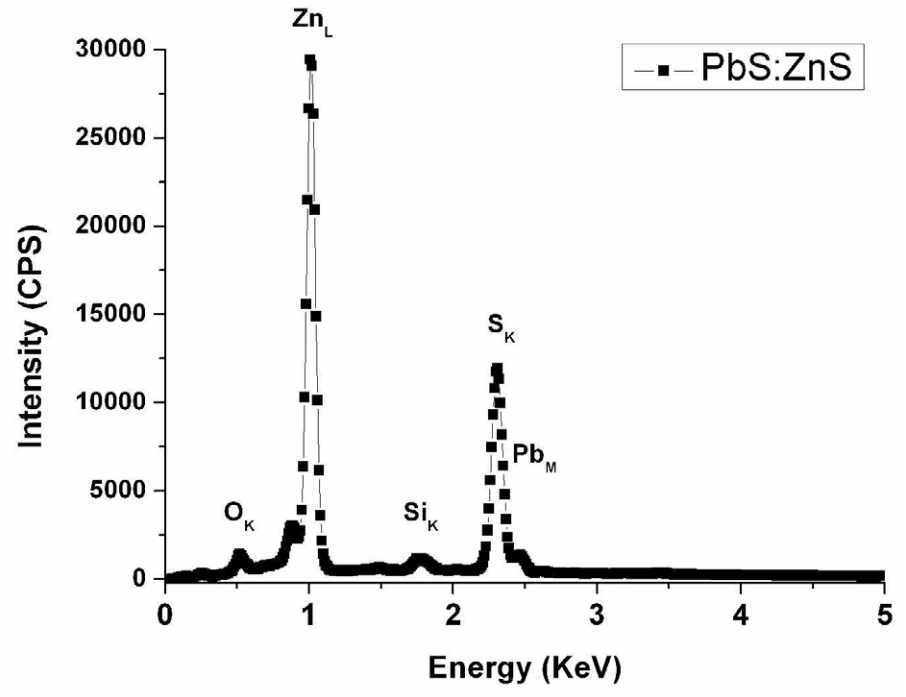


Fig. 6. EDX spectra for PbS:ZnS film deposited on Si(100) substrate.

Table 2. Weight and Atomic percentage for PbS:ZnS film

| Element | Weight % | Atomic % |
|---|---|---|
| O K | 1.8 | 5.72 |
| Zn L | 66.16 | 51.46 |
| S K | 26.08 | 41.36 |
| Pb M | 5.96 | 1.46 |

ZnS polycrystalline was cubic structural using electron gun deposition, this difference in phase (cubic or hexagonal) could be due to the nature of the deposition methods (bombardment energy, physics or chemistry of precursors).

Photoluminance (PL) emission spectrum characterization at room temperature of PbS:ZnS film is shown in Fig. 7-c. It show another peaks at 482 nm and 498 nm correspond to the defects in the film (transition of electrons to sulfur vacancies) ; it is known that in nanocrystals, as the size of the crystal is reduced, PL peaks shift toward to shorter wavelength [39]. The small peak centered at 380 nm can corresponds to the ZnO; where the O is contamination for nanowires.

*UV study*

Fig. 8-a shows the UV transmissions spectrum for ZnS film (0 wt% PbS), It has an average transmittance of samples deposited on glass substrate in the visible range about 95%. However, it has reduces to 50 % with Pb doping concentration (8-a). The band gap was about 3.52 eV for non doped film (Fig. 8-b) and it was about 3.32 eV for PbS:ZnS nanowires (doped film).

This variation in band gap value due to the structural different (nanowires for doped one and dense for non doped film) and to the dopant element (PbS as dopant for nanowires film). Also, the behavior of decreasing the band gap with the PbS doping could be attributed to an enhancement of the crystalline quality and it cited in or recent work [39].

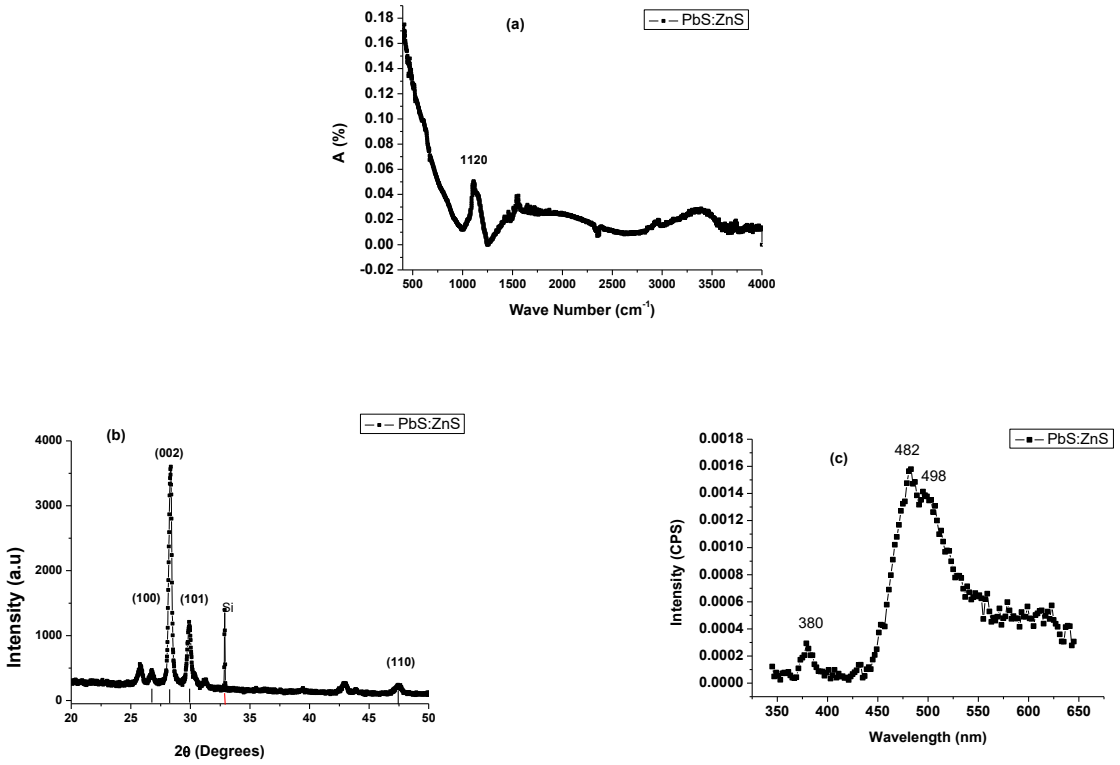


Fig. 7. (a) FTIR spectrum, (b) XRD pattern and (c) PL spectrum for ZnS nanowires film deposited on Si substrate.

Table 3. FTIR peaks for PbS:ZnS film

| Materials | Peak ($cm^{-1}$) |
|---|---|
| ZnS | 1120 |
| humidity | 1535 |
| Si | 2350 |

## CONCLUSION

In this paper, ZnS nanowires (NWs) have been prepared using simple thermal evaporation method and deposited on silicon and glass substrates. The optical and structural properties of the obtained samples have been studied using XRD, HRTEM, and PL techniques. HRTEM, AFM, and SEM studies have shown that the surface of NWs is very smooth, the diameter of the obtained nanowires is about 50 nm, and the length is several micron. EDX with SEM, and TEM techniques have confirmed that the films were stoichiometry. UV-Vis spectra were used to obtain the band gap of the PbS;ZnS nanowires as well as ZnS nandoped (ZnS) deposited on glass substrate. XRD, FTIR, and PL study have confirmed the Nanostructural of the deposited film**.** The transmittance in the visible spectra range, energy band gaps, and the electrical properties of obtained ZnS samples will be investigated in our future work to confirm the viability of Pb:ZnS samples for gas sensing and/or solar cell applications.

## ACKNOWLEDGMENTS

The authors greatly acknowledge funds to this project by Professor I. Othman, the Director General of the Atomic Energy Commission of Syria, Dr M. Zidan for beneficial discussions and Dr G. Patriarche and Dr A. Soltani for HRTEM

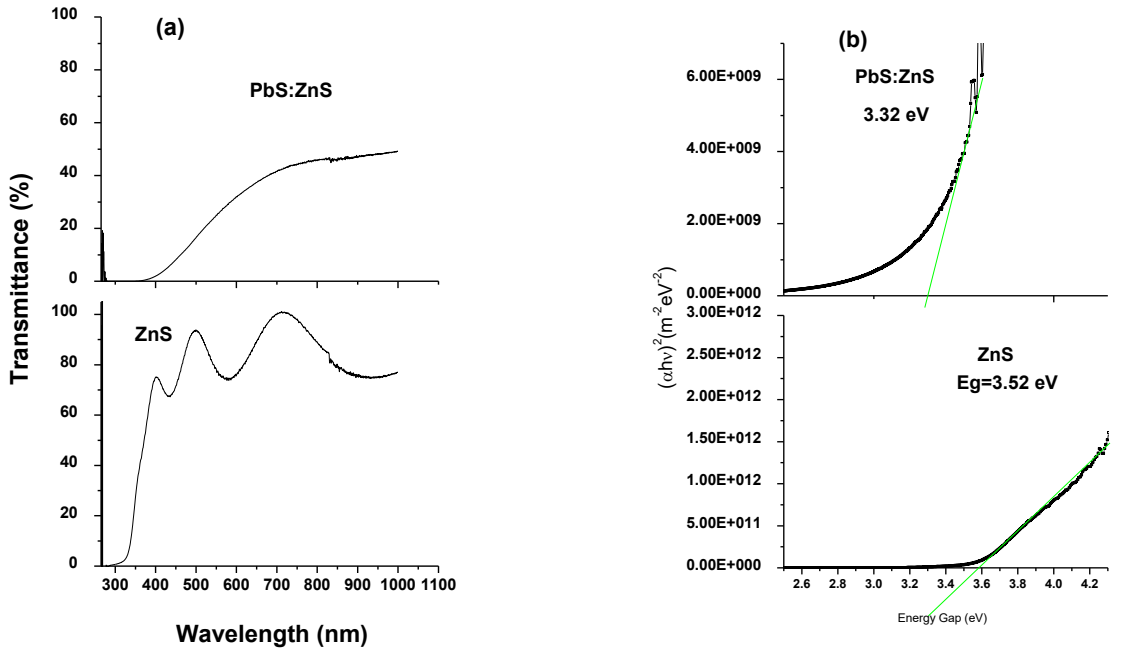


Fig. 8. (a) UV-Vis Optical transmittance spectra for undoped film (0 wt%) and doped film (6 wt%) and(b) corresponding band gap for two films ZnS.

measurements.

## CONFLICT OF INTEREST

The authors declare that there is no conflict of interests regarding the publication of this manuscript.

## REFERENCES


1. Haque F, Rahman KS, M. A. Islam MJR, Akhtaruzzaman M, Alam MM, Alothman ZA, et al. Growth optimization of ZnS thin films by RF magnetron sputtering as prospective buffer layer in thin film solar cells. Chalcogenide Letters. 2014;11(4):189-197.
2. Shin SW, Pawar SM, Park CY, Yun JH, Moon J-H, Kim JH, et al. Studies on Cu2ZnSnS4 (CZTS) absorber layer using different stacking orders in precursor thin films. Solar Energy Materials and Solar Cells. 2011;95(12):3202-6.
3. Abdallah B, Zidan MD, Allahham A. Syntheses, Structural and Nonlinear Optical Characteristics of ZnO Films Using Z-Scan Technique. Silicon. 2020.
4. Sorinezami Z, Ghanbari D. Facile preparation of silver nanoparticles and antibacterial Chitosan-Ag polymeric nanocomposites. Journal of Nanostructures. 2019;9(3):396-401.
5. Bagheri A, Halakouie H, Ghanbari D, Mousayi M, Asiabani N. Strontium hexa-ferrites and polyaniline nanocomposite: Studies of magnetization, coercivity, morphology and microwave absorption. Journal of Nanostructures. 2019;9(4):630-638.
6. Eskandari N, Nabiyouni G, Masoumi S, Ghanbari D. Preparation of a new magnetic and photo-catalyst CoFe2O4–SrTiO3 perovskite nanocomposite for photo-degradation of toxic dyes under short time visible irradiation. Composites Part B: Engineering. 2019;176:107343.
7. Nabiyouni G, Ghanbari D. Simple preparation of magnetic, antibacterial and photo-catalyst $NiFe_2O_4$@$TiO_2$/Pt nanocomposites. Journal of Nanostructures. 2018;8(4):408-416.
8. Ao D, Ichimura M. UV irradiation effects on hydrogen sensors based on SnO2 thin films fabricated by the photochemical deposition. Solid-State Electronics. 2012;69:1-3.
9. Chaisitsak S. Nanocrystalline SnO2:F Thin Films for Liquid Petroleum Gas Sensors. Sensors. 2011;11(7):7127-40.
10. Abdelkrim A, Rahmane S, Abdelouahab O, Abdelmalek N, Brahim G. Effect of solution concentration on the structural, optical and electrical properties of SnO2 thin films prepared by spray pyrolysis. Optik. 2016;127(5):2653-8.
11. Yousefi R, Jamali-Sheini F, Sa'aedi A, Zak AK, Cheraghizade M, Pilban-Jahromi S, et al. Influence of lead concentration on morphology and optical properties of Pb-doped ZnO nanowires. Ceramics International. 2013;39(8):9115-9.
12. Lin Y-C, Chao Y-T, Yao P-C. Influence of humidity on the growth characteristics and properties of chemical bath-deposited ZnS thin films. Applied Surface Science. 2014;307:724-30.
13. Sinha T, Lilhare D, Khare A. Effects of Various Parameters on Structural and Optical Properties of CBD-Grown ZnS Thin Films: A Review. Journal of Electronic Materials. 2017;47(2):1730-51.
14. Kurnia F, Ng YH, Tang Y, Amal R, Valanoor N, Hart JN. ZnS Thin Films for Visible-Light Active Photoelectrodes: Effect

of Film Morphology and Crystal Structure. Crystal Growth & Design. 2016;16(5):2461-5.
15. Abdallah B, Zidan MD, Allahham A. Deposition of ZnS films by RF magnetron sputtering: Structural and optical properties using Z-scan technique. International Journal of Modern Physics B. 2019;33(29):1950348.
16. Vishwakarma K, Vishwakarma OP, Pandey SK, Ramrakhiani M. Synthesis and Photoluminescence Studies on Nanocrystalline Content Zns Film International Journal of Pure and Applied Physics 2010;6(2):143–149.
17. Alnama K, Abdallah B, Kanaan S. Deposition of ZnS thin film by ultrasonic spray pyrolysis: effect of thickness on the crystallographic and electrical properties. Composite Interfaces. 2016;24(5):499-513.
18. Vishwakarma R. Effect of substrate temperature on ZnS films prepared by thermal evaporation technique. Journal of Theoretical and Applied Physics. 2015;9(3):185-92.
19. Jeyachitra R, Senthilnathan V, Kathirvel D. Optical, Photoluminescence and Electrical properties of Vacuum evaporated ZnS thin films. International Journal of ChemTech Research. 2014;6(5):3152-3159.
20. Al-Douri AAJ, Heavens OS. The influence of deposition parameters on the optical properties and growth of ZnS films. Thin Solid Films. 1983;100(4):273-81.
21. Bendjedidi H, Attaf A, Saidi H, Aida MS, Semmari S, Bouhdjar A, et al. Properties of n-type SnO2 semiconductor prepared by spray ultrasonic technique for photovoltaic applications. Journal of Semiconductors. 2015;36(12):123002.
22. Abdallah B, Kakhia M, Abou Shaker S. Deposition of Na2WO4films by ultrasonic spray pyrolysis: effect of thickness on the crystallographic and sensing properties. Composite Interfaces. 2016;23(7):663-74.
23. MoteI VD, Purushotham Y, Dole BN. Structural, morphological and optical properties Mn-ZnS. Cerâmica. 2013; 59 614-619.
24. Vaishnav VS, Patel PD, Patel NG. Indium Tin Oxide thin film gas sensors for detection of ethanol vapours. Thin Solid Films. 2005;490(1):94-100.
25. Hazra P, Singh SK, Jit S. Impact of surface morphology of Si substrate on performance of Si/ZnO heterojunction devices grown by atomic layer deposition technique. Journal of Vacuum Science & Technology A: Vacuum, Surfaces, and Films. 2015;33(1):01A114.
26. Abdallah B, Alnama K, Nasrallah F. Deposition of ZnS thin films by electron beam evaporation technique, effect of thickness on the crystallographic and optical properties. Modern Physics Letters B. 2019;33(04):1950034.
27. Moore D, Ding Y, Wang ZL. Hierarchical Structured Nanohelices of ZnS. Angewandte Chemie International Edition. 2006;45(31):5150-4.
28. Yu JH, Joo J, Park HM, Baik S-I, Kim YW, Kim SC, et al. Synthesis of Quantum-Sized Cubic ZnS Nanorods by the Oriented Attachment Mechanism. Journal of the American Chemical Society. 2005;127(15):5662-70.
29. Malyarevich AM, Gaponenko MS, Savitski VG, Yumashev KV, Rachkovskaya GE, Zakharevich GB. Nonlinear optical properties of PbS quantum dots in boro-silicate glass. Journal of Non-Crystalline Solids. 2007;353(11-12):1195-200.
30. D'Amico P, Calzolari A, Ruini A, Catellani A. New energy with ZnS: novel applications for a standard transparent compound. Scientific Reports. 2017;7(1).
31. Ahmad M, Pan C, Yan W, Zhu J. Effect of Pb-doping on the morphology, structural and optical properties of ZnO nanowires synthesized via modified thermal evaporation. Materials Science and Engineering: B. 2010;174(1-3):55-8.
32. Sahoo SK, Mangal S, Mishra DK, Singh UP, Kumar P. 50 keV H+ion beam irradiation of Al doped ZnO thin films: Studies of radiation stability for device applications. Surface and Interface Analysis. 2017;49(12):1279-86.
33. Lin Y-R, Yang S-S, Tsai S-Y, Hsu H-C, Wu S-T, Chen IC. Visible Photoluminescence of Ultrathin ZnO Nanowire at Room Temperature. Crystal Growth & Design. 2006;6(8):1951-5.
34. Gokarna A, Parize R, Kadiri H, Nomenyo K, Patriarche G, Miska P, et al. Highly crystalline urchin-like structures made of ultra-thin zinc oxide nanowires. RSC Adv. 2014;4(88):47234-9.
35. Sun Y, George Ndifor-Angwafor N, Jason Riley D, Ashfold MNR. Synthesis and photoluminescence of ultra-thin ZnO nanowire/nanotube arrays formed by hydrothermal growth. Chemical Physics Letters. 2006;431(4-6):352-7.
36. Shkurmanov A, Sturm C, Franke H, Lenzner J, Grundmann M. Low-Temperature PLD-Growth of Ultrathin ZnO Nanowires by Using Zn x Al1−x O and Zn x Ga1−x O Seed Layers. Nanoscale Research Letters. 2017;12(1).
37. Alnama K, Abdallah B, Kanaan S. Deposition of ZnS thin film by ultrasonic spray pyrolysis: effect of thickness on the crystallographic and electrical properties. Composite Interfaces. 2016;24(5):499-513.
38. Jazmati AK, Abdallah B, Lahlah F, Abou Shaker S. Photoluminescence and optical response of ZnO films deposited on silicon and glass substrates. Materials Research Express. 2019;6(8):086401.
39. Abdallah B, Kakhia M, Zetoune W. Structural, optical and sensing properties of ZnS thick films deposited by RF magnetron sputtering technique at different powers. World Journal of Engineering. 2020;17(3):381-8.